

Highly Sensitive Ammonia Sensor with Organic Vertical Nanojunctions for Noninvasive Detection of Hepatic Injury

Ming-Zhi Dai,^{†,¶} Yi-Lo Lin,^{‡,§,¶} Hung-Cheng Lin,^{||} Hsiao-Wen Zan,^{*,||} Kai-Ting Chang,^{§,⊥} Hsin-Fei Meng,[†] Jiunn-Wang Liao,[‡] May-Jywan Tsai,[§] and Henrich Cheng^{*,§,⊥,▽,○}

[†]Institute of Physics, National Chiao Tung University, Hsinchu, Taiwan

[‡]Graduate Institute of Veterinary Pathobiology, College of Veterinary Medicine, National Chung Hsing University, Taichung, Taiwan

[§]Neural Regeneration Laboratory, Department of Neurosurgery, Neurological Institute, Taipei Veterans General Hospital, Taipei, Taiwan

^{||}Department of Photonics, National Chiao Tung University, Hsinchu, Taiwan

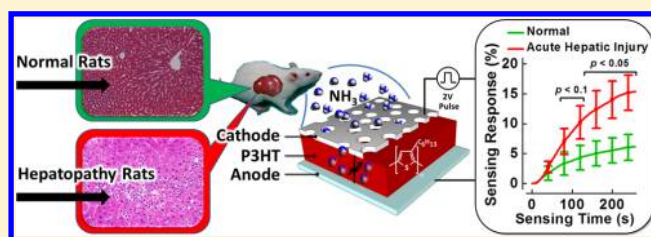
[⊥]Department and Institute of Pharmacology, School of Medicine, National Yang-Ming University, Taipei, Taiwan

[▽]Center for Neural Regeneration, Department of Neurosurgery, Neurological Institute, Taipei Veterans General Hospital, Taipei, Taiwan

[○]Brain Research Center, School of Medicine, National Yang-Ming University, Taipei, Taiwan

Supporting Information

ABSTRACT: We successfully demonstrate the first solid-state sensor to have reliable responses to breath ammonia of rat. For thioacetamide (TAA)-induced hepatopathy rats, we observe that the proposed sensor can detect liver that undergoes acute–moderate hepatopathy with a p -value less than 0.05. The proposed sensor is an organic diode with vertical nanojunctions produced by using low-cost colloidal lithography. Its simple structure and low production cost facilitates the development of point-of-care technology. We also anticipate that the study is a starting point for investigating sophisticated breath-ammonia-related disease models.



In exhaled breath, ammonia odor could be linked to liver and kidney malfunction.^{1–5} In chronic liver disorder, it is usually asymptomatic until its late stages. Therefore, it is recommended for patients with hepatitis history or carriers of hepatitis virus to monitor liver function regularly. Since early fibrotic changes are reversible, the prognosis of fibrosis can be improved if diagnosed early and may lower the risk of the development of severe conditions such as cirrhosis or cancer. Because the damage of hepatocytes leads to an increase in blood-ammonia levels (hyperammonemia), the breath of these patients may have an ammonia-like odor.^{1–5} (See Supporting Information: Generation of Breath Ammonia.) Monitoring liver disease by detecting breath ammonia is thus one critical issue when developing point-of-care technology.⁶ Another condition that may have an ammonia-like odor is in patients with kidney diseases, especially in the end stage of renal failure. In previous reports, breath ammonia has been shown to be useful to determine efficacy and end point of hemodialysis for patients with end-stage renal disease.⁷ Besides, breath ammonia has also been demonstrated as a biomarker for *Helicobacter pylori* and oral cavity disease.^{7–9}

Instruments using mass spectrometry,^{4,7,10} optical settings,^{11,12} or quartz crystal microbalance^{13,14} system have been successfully demonstrated to reliably detect breath ammonia. However, a simple, reliable, portable, and low-cost breath ammonia sensor is still not commercialized, hence limiting its

development for point-of-care applications.⁶ The comparison between various kinds of ammonia sensors is in Supporting Information Tables S-1 and S-2.^{7,10–20} Since breath ammonia reflects several diseases like hepatic disease, renal failure, *H. pylori*, and oral cavity disease, breath ammonia itself cannot be used as a biomarker to identify the disease. Rather, it could provide a kind of health alert to encourage following detailed examinations in hospital or could trace patients' condition at home as point-of-care applications. Breath ammonia can also serve as part of a breath fingerprint to form a sensing map together with other targeting species such as volatile organic compounds (VOCs) in exhaled breath.^{21–24}

In this work, a novel and sensitive breath ammonia sensor based on organic semiconductor material is successfully demonstrated. It has been recognized that organic thin-film transistors (OTFTs) can be used as gas sensors to detect various kinds of gas molecules.²⁵ Low-cost fabrication of organic-based electronics also facilitates the development of disposable sensors for medical applications. The organic semiconductors of OTFTs are exposed to analytes, and the channel currents are changed by

Received: October 23, 2012

Accepted: February 8, 2013

Published: February 8, 2013

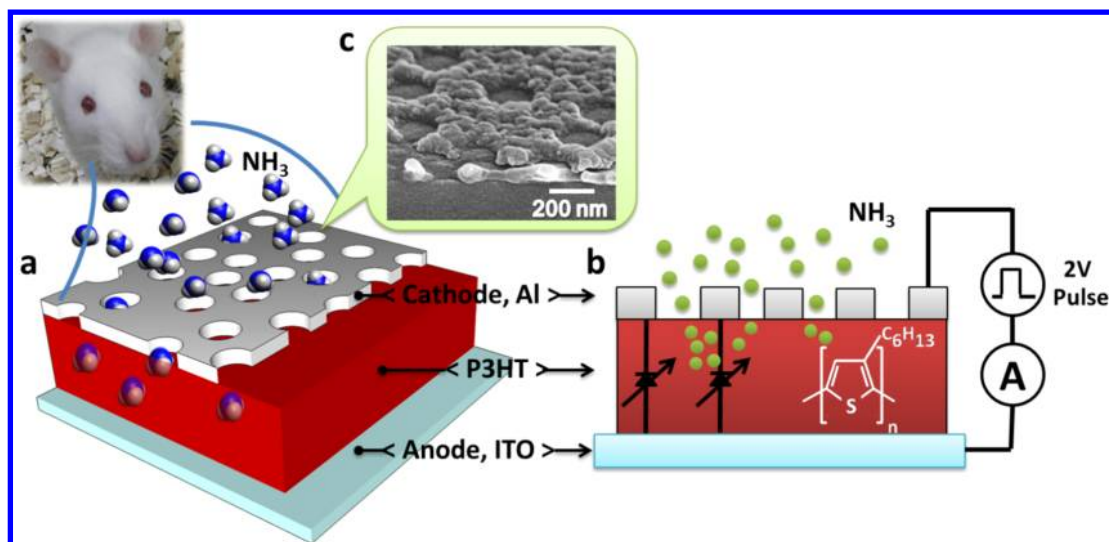


Figure 1. (a) Three-dimensional and (b) two-dimensional schematic structures of the proposed ammonia sensor, the VNJ-P3HT diode. The molecular structure of P3HT and the equivalent parallel-connected vertical diodes are shown inside panel b. (c) The scanning electron microscope image of the VNJ-P3HT diode.

charge doping or dedoping due to the analytes. However, the limit of the lowest detection (LOD) of an OTFT-based ammonia sensor is in the part-per-million (ppm) range.¹⁸ To detect breath ammonia, a sensing system with high selectivity and an LOD lower than 50 ppb (parts per billion) is required.^{6,26} Here we propose an ammonia sensor based on an organic diode with vertical nanojunctions (VNJ) to exhibit reliable responses to breath ammonia of rats. The proposed ammonia sensor has an LOD lower than 20 ppb, a real-time response, a good enough selectivity, a simple structure, a high reproducibility, and a low production cost. We used the proposed sensor to directly detect the breath ammonia of rat. Reliable responses were obtained in over 240 trials using over 80 sensing devices. In this study, we used a hepatopathy animal model to exam the sensor. For thioacetamide (TAA)-induced hepatopathy rats,^{27,28} we first observe that a solid-state sensor can reflect liver that undergoes moderate hepatopathy with a *p*-value less than 0.05. (Kruskal–Wallis one-way ANOVA with Dunn’s post hoc analysis.) It is noted that commercial carbon dioxide (CO₂) absorber and cooling system are used to remove CO₂ and to reduce the relative humidity (i.e., RH < 10%). The device malfunction due to CO₂ and the signal shifting due to water molecules will be discussed.

■ MATERIALS AND METHODS

Novel Organic Diode-Like Sensors with Vertical Nanojunctions. The three-dimensional and two-dimensional structures of the proposed solid-state ammonia sensor are shown in Figure 1, parts a and b, respectively. A vertical organic diode with a porous top electrode is fabricated. From bottom to top, a simple anode/semiconductor/cathode sandwich structure is formed by using indium tin oxide (ITO)/regioregular poly(3-hexylthiophene) (P3HT)/aluminum (Al). P3HT is a kind of *p*-type solution-processed polymer semiconductor material and is the ammonia sensing layer in the proposed sensor. According to many previous reports, ammonia molecules act like acceptors to dedope P3HT material.^{18,29} To facilitate the interaction between gaseous ammonia molecules and P3HT film, high-density nanometer pores are produced on the cathode by using a low-cost colloidal lithography process.^{16,30} The scanning electron microscope (SEM) image of the produced sensor is shown in

Figure 1c. The proposed sensor can be represented by an equivalent circuit as shown in Figure 1b. Numerous vertical diodes, named as the vertical nanojunctions (VNJ), are connected in parallel. Ammonia molecules react with these connected P3HT diodes by diffusing into P3HT film through the high-density pores, dedoping the P3HT film, and reducing the diode current.

Low-Cost Nanostructure Fabrication with Self-Organized Colloidal Lithography. The schematic diagrams and the corresponding SEM images of the key process steps when fabricating the proposed P3HT diode with vertical nanojunctions (VNJ-P3HT diode) are shown in Figure 2. The vertical sensors with active area as 1 mm² were fabricated on indium tin oxide glass substrate treated by a 100 W oxygen plasma for 15 min. A solution of 2.5 wt % P3HT (Rieke Metals) dissolved in chlorobenzene was spun coated on substrate to form a 60 nm thick P3HT layer. After the P3HT film was annealed at 200 °C for 10 min, the thin-film P3HT was spin rinsed with *p*-xylene. Then the substrate was submerged into dilute ethanol solution of 200 nm negatively charged polystyrene (PS) spheres (Fluka) with 0.24 wt % for 40 s. Some of PS spheres were adsorbed on the substrate as the shadow mask. The wet substrate was dipped into boiling isopropyl alcohol (IPA) for 10 s. After dipping into IPA, the substrate was blow-dried immediately. As shown in Figure 2a, high-density self-organized polystyrene spheres with diameter as 200 nm were absorbed onto P3HT. Aluminum of 40 nm was deposited as the metal electrode by a thermal evaporation coater as shown in Figure 2b. We used adhesive tape (Scotch, 3M) to remove the PS spheres. The aluminum cathode with high-density nanopores was formed as shown in Figure 2c.

Animals and Histological Evaluation in Liver Tissue. Adult female Sprague–Dawley rats (225–250 g) were used in this study. All procedures involving animals were reviewed and approved by the Institutional Animal Care and Use Committee of Taipei Veterans General Hospital, Taiwan. The rats with induced hepatic injury were randomly assigned to two treatment groups: acute group (*n* = 5) or chronic group (*n* = 8). In the acute group, hepatic failure was induced by intraperitoneal (ip) injection of 350 mg/kg/day of TAA for 3 days.²⁷ In the chronic

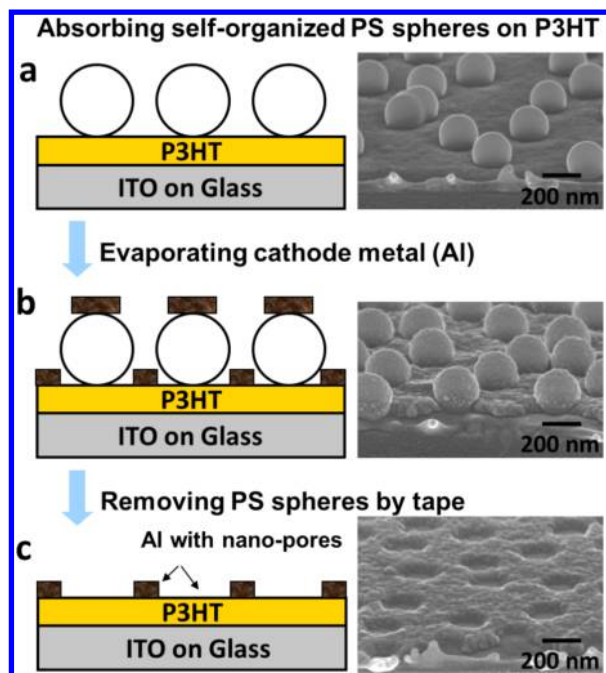


Figure 2. Schematic diagrams and the corresponding SEM images of the key process steps when fabricating VNJ-P3HT diodes. (a) High-density self-organized polystyrene spheres with diameter as 200 nm are absorbed onto P3HT. (b) Aluminum of 40 nm was deposited as the metal electrode by a thermal evaporation coater. (c) Aluminum cathode with high-density nanopores is formed.

group, 0.03% TAA was administrated in drinking water for 21 or 35 days.²⁸ Breath ammonia was measured 1 day before animals were sacrificed. Animals were sacrificed at day 7 for the acute group and at day 21 or 35 for the chronic groups, respectively. Deparaffinized sections (4 μm) of liver tissue was stained using standard H&E staining for the histological evaluation.

Microfluid System to Detect Ammonia with Known Concentrations. Here, the sensor responses in two kinds of backgrounds are tested. In the first case, as shown in Figure 3a, the VNJ-P3HT diode was placed in a microfluid sensing chamber containing a high-purity (99.9999%) nitrogen gas (N_2). The test gases selected from several common elements of breathing gas were prepared from a 100 ppm ammonia (NH_3) cylinder (purity,

99.9995%), 100 ppm acetone cylinder (purity, 99.99%), 1% nitric oxide (NO) cylinder (purity, 99.999%), carbon dioxide cylinder (purity, 99.999%), and absolute ethanol. The gaseous ethanol was precollected by mixing saturated vapor and N_2 . We used an electrical syringe pump (NH_3 , acetone, and gaseous ethanol), mass-flow controller (NO), and flow meter (CO_2) to inject the test gas into a tube to mix with the high-purity nitrogen gas. The gas mixture then entered the microfluid system. The nitrogen gas flow was controlled by a mass-flow controller (MFC), and specific concentrations of test gas (NH_3 , acetone, and gaseous ethanol) were obtained by adjusting the injection speed of the syringe pump. The current of the VNJ-P3HT diode was measured by a Keithley SourceMeter (models 2400 and 2602), and the voltage bias of the VNJ-P3HT diode was provided by 2 V pulse cycles (80 ms pulse width and 1 s period).

In the second case, as shown in Figure 3b, sensors are measured with ambient background. Reaction between water molecules and P3HT causes a continuous current increase and thus degrades the sensor sensitivity to ammonia. CO_2 molecules are also found to destroy sensor function (details will be discussed in the Sensor Selectivity section). Hence, humidity and CO_2 concentration need to be suppressed. Relative humidity (RH) is reduced to be lower than 10% by introducing ambient air through a 7 m tube at -20°C . A commercial CO_2 absorber, which contained sodium hydroxide coated silica particles, was added into the sensing system without affecting the ammonia sensing response. To verify that the response is due to ammonia, the sensing tube can be switched to connect with an ammonia filter ($\text{NiCl}_2 \cdot 6\text{H}_2\text{O}$ powders) before entering the sensing chamber. Various concentrations of the test gases were obtained by injecting various volumes of target gas into a box.

Microfluid System (with Low Humidity and Low CO_2 Concentration) for Real-Time Rats' Breath Testing. As shown in Figure 3b, the VNJ-P3HT diode was placed in a microfluid sensing chamber containing a background ambient air. As aforementioned, dry air (RH < 10%) was controlled by introducing the collecting air through a 7 m tube at -20°C and CO_2 concentration is suppressed by inserting a commercial CO_2 absorber into the system. We used a mask to cover the nose (as well as mouth) of rats when detecting breath ammonia or to contact ambient when not detecting breath ammonia. The output end of the microfluid system is connected with a pump. The pumping flow is fixed as 2 NL/min. The current of the VNJ-

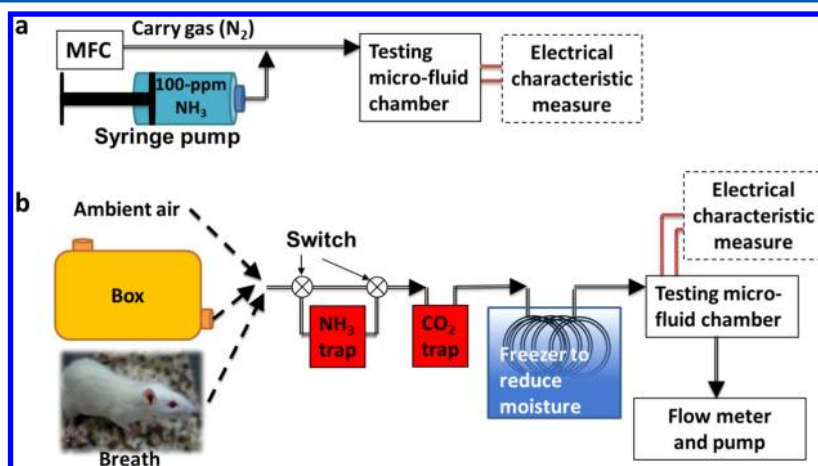


Figure 3. Schematic diagrams of (a) the sensing system to detect ammonia when the background is pure nitrogen and (b) the sensing system to detect ammonia or breath ammonia when the background is ambient air.

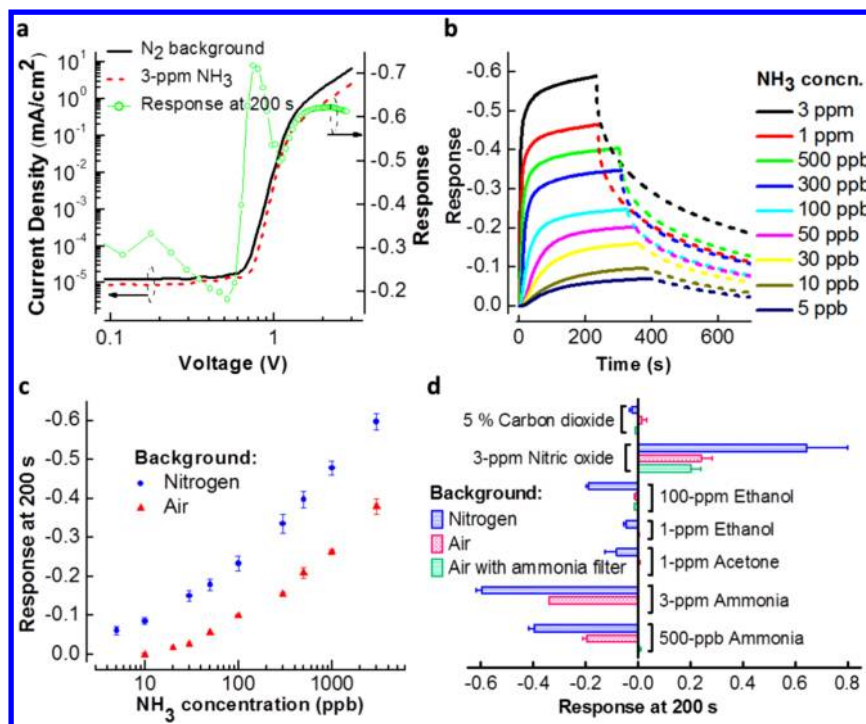


Figure 4. (a) J - V curve of VNJ-P3HT diodes before (black solid curve) and after 200 s of 3 ppm ammonia sensing (red dashed curve). Green symbols represent the response (i.e., the current variation ratio) of VNJ-P3HT diodes. (b) With pure nitrogen as the background, the responses (defined as the current variation ratio) as a function of time after injecting ammonia with various concentrations and after removing ammonia are shown by solid lines and dashed lines, respectively. (c) The response (measured at 2 V with a fixed sensing time as 200 s) as a function of ammonia concentration. Backgrounds are pure nitrogen and dry air (RH < 10%). The data with standard deviations are obtained from at least 30 independent measurements by using more than 13 devices. (d) The responses (measured at 2 V with a fixed sensing time as 200 s) to carbon dioxide (5%), nitric oxide (3 ppm), ethanol (100 and 1 ppm), acetone (1 ppm), and ammonia (3 ppm and 500 ppb). Blue bars, red bars, and green bars represent responses with backgrounds as pure nitrogen, dry air, and dry air passing through commercial ammonia filter (NiCl₂·6H₂O powders).

P3HT diode is measured by 2 V pulse cycles (80 ms pulse width and 1 s period), and the voltage bias of the VNJ-P3HT diode is provided by Keithley SourceMeter (models 2400 and 2602). The reason to use a high flow rate in this study is to increase sensor response when ammonia concentration is low (i.e., <100 ppb). We found that, when ammonia concentration is high (i.e., 500 ppb), changing the flow rate from 2 to 0.6 NL/min does not change the response read at 200 s. When ammonia concentration is low (i.e., 50 ppb), changing flow rate from 2 to 0.6 NL/min causes about 30% drop of the response read at 200 s (data not shown). It is plausible that the high flow rate can reduce system loss and can maintain high diffusion flux for ammonia to diffuse into P3HT. Further investigation is required to understand the flow rate effect. To verify that the sensing signal is related to breath ammonia, we utilize a commercial ammonia filter to check if the sensing response is eliminated or not. Also, we access two kinds of independent measurement methods to analyze the breath of normal rat and the breath of rat with liver injury. The first method is ion chromatography/conductivity detection (IC, DX-100 from Dionex) to analyze ammonia concentration in rats' breath.³¹ We can distinguish whether the breath ammonia concentration is higher than 100 ppb or not. The second method is gas chromatography/mass spectroscopy (GC/MS, 6890 gas chromatograph and 5973 mass selective detector, both from Hewlett-Packard) to analyze the components and concentrations of volatile organic compounds (VOCs) in rats' breath.³²

RESULTS

Electrical Properties of the VNJ-P3HT Diode before and during Ammonia Sensing.

Before measuring the ammonia sensing response, we first investigate the original characteristics of the VNJ-P3HT diode. The current density as a function of applied bias (J - V curves) of the VNJ-P3HT diode is shown in Figure 4a. It is observed that the current density is proportional to the square of the applied bias, indicating that holes in P3HT follow the space-charge-limited conduction (SCLC).³³ It is well-known that carrier transport in most intrinsic or low-doped conjugated polymers follows the space-charge-limited current.³⁴ The injected charge carrier density is much higher than the background doping density in most volume of the sample (i.e., in the bulk region). The injected charges are considered as space charges because they are unipolar carriers with very low mobility. Most of the injected charges accumulate close to the injection interface. Away from the injection interface, the charge density decreases.

Then, we put the VNJ-P3HT diode into the sensing system to analyze its ammonia sensing behavior. After injecting the 3 ppm ammonia (with a background of nitrogen) for 200 s, the J - V curve of the VNJ-P3HT diode is shown by the red dashed line in Figure 4a. The slightly right shift of the onset voltage indicates a small increase of hole injection barrier after exposure to ammonia. The main response, however, is the current drop in the SCLC region. We use the current variation ratio, which is the current difference divided by the initial current, to represent the response of the sensor. The response to a 200 s 3 ppm ammonia exposure is plotted as a function of applied bias by the green

symbols in Figure 4a. A response peak is obtained at around 0.8 V; however, the diode current at 0.8 V is too low to provide a good signal-to-noise ratio. When the applied bias changes from 1.5 to 3 V, a large and stable response as -0.6 is obtained. In the following works, we choose 2 V as a fixed applied bias to measure the response.

Sensor Response to Ammonia. After analyzing the J - V curve variation during ammonia sensing as described in Figure 4a, the response of the sensor is defined as the current variation ratio measured at 2 V. The sensing responses after injecting ammonia (shown by solid lines) and the recovery responses after removing ammonia (shown by dashed lines) are plotted as a function of time in Figure 4b. With a fixed reading time at 200 s, response as a function of ammonia concentration is plotted in Figure 4c. The data with standard deviations are obtained from 70 independent measurements by using 13 devices. An LOD as 5 ppb can be obtained when the background is pure nitrogen. When we use the VNJ-P3HT diode to detect the mixture of ammonia and ambient air, we still obtain reliable and repeatable responses (shown by red symbols in Figure 4c; standard deviations are obtained from 30 independent measurements by using 18 devices) with an LOD as 20 ppb after reducing the relative humidity to be lower than 10% and filtering out carbon dioxide. The less sensitive performance with ambient background may be due to the following reasons. First, oxygen and the remaining water molecules cause a slight shift of background current and hence interfere the readability of current response to ammonia. Second, the remaining water molecules on the tube increase the absorption of ammonia molecules on tube sidewall and hence reduce ammonia concentrations.

Sensor Selectivity. We also analyze the responses of the VNJ-P3HT diode to several kinds of gases existing in human breath.^{1,6} In Figure 4d, we compare the response of the VNJ-P3HT diode (measured at 2 V with a fixed sensing time as 200 s) to carbon dioxide (5%), nitric oxide (3 ppm), ethanol (100 and 1 ppm), acetone (1 ppm), and ammonia (3 ppm and 500 ppb). Blue bars, red bars, and green bars represent responses with backgrounds as pure nitrogen, dry air, and dry air passing through commercial ammonia filter ($\text{NiCl}_2 \cdot 6\text{H}_2\text{O}$ powders). With dry air as the background, the VNJ-P3HT diode has very small responses (0.009 to -0.017) to ethanol and acetone. The significantly suppressed response to ethanol and acetone in dry air may be due to the greatly suppressed vapor pressure of ethanol (2 mmHg) and acetone (20 mmHg) at -20 °C. In other words, cooling the tube at -20 °C before connecting to the sensor device (i.e., the sensor is at room temperature) leads to a suppressed humidity and suppressed concentrations of VOCs. The boiling point of ammonia is -33.3 °C; the concentration of ammonia should not be significantly altered in our system. The response to 3 ppm nitric oxide, on the other hand, is positive and significant. The response is known to be due to the oxidation (doping) of P3HT^{35,36} and is not reversible. Thankfully, as aforementioned, we only have a very low concentration (<40 ppb) of nitric oxide in our breath.⁶ In Supporting Information Figure S-1a, we also show that ammonia-induced dedoping reaction dominates the sensor response when 200 ppb NH_3 (electron donors)^{18,29} and 100 ppb NO (electron acceptors)^{35,36} molecules coexist. The response to 5% CO_2 is smaller than ± 0.06 . However, as shown in Supporting Information Figure S-1b, CO_2 molecules significantly degrade the sensor's response to ammonia when CO_2 and ammonia coexist (dark blue line in Supporting Information Figure S-1b). Moreover, after being exposed to CO_2 , the device has a severely degraded response to

ammonia (light blue line in Supporting Information Figure S-1b). It is known that CO_2 molecules easily dissolve in water to form acetic acid. It is possible that the formation of acid on P3HT readily destroys the film structure and the diode characteristics. A commercial CO_2 absorber, which contains sodium hydroxide coated silica particles, is then added into the sensing system without affecting the ammonia sensing response (red line and green line in Supporting Information Figure S-1b). Finally, after reducing humidity ($\text{RH} < 10\%$) and removing CO_2 by using the commercial CO_2 trapping nanoparticles (sodium hydroxide coated silica particles) as shown in Figure 3b, we obtain stable and repeatable ammonia response in the breath of rat as shown in Supporting Information Figure S-2.

Detecting Breath of Rats. The sensing system with VNJ-P3HT diodes is then used to detect breath of three groups of rats: normal rats ($n = 11$, denoted by N1–N11), rats with induced acute hepatic injury ($n = 5$, acute group, denoted by A1–A5), and rats with induced chronic hepatic injury ($n = 8$, chronic group, denoted by C1–C8). Breath ammonia was measured 1 day before animals were sacrificed. Acute group rats were sacrificed at day 7. Chronic group rats were sacrificed at day 21 (C1–C4) and 35 (C5–C8). Sensor responses measured at 2 V with a 200 s breath exposure of these animals are shown in Figure 5. The

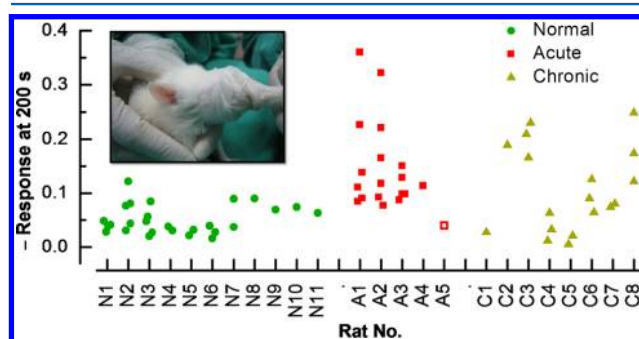


Figure 5. Sensor responses measured at 2 V with a 200 s breath exposure for three groups of rats: normal rats (N1–N11), rats with induced acute hepatic injury (A1–A5), and rats with induced chronic hepatic injury (C1–C8). Inset: photo to show the breath collecting by using a mask to cover the rat's nose and mouth.

absolute value of the responses of rats in the acute group (red symbols) are large (mostly between 0.08 and 0.22), while those of rats in the normal group (green symbols) are small (between 0.02 and 0.13). A5 in the acute group exhibits a particularly small response value (0.05). Chronic groups sacrificed at day 21 and day 35 deliver similar responses to VNJ-P3HT diodes. The absolute value of the responses of rats in the chronic group (yellow symbols) ranges from 0.02 to 0.21. The sensor responses obtained from one single rat have a large deviation. We will discuss the large deviation in the Discussion session. Here, it is noted that only rats with liver injury (both acute and chronic) deliver response with an absolute value larger than 0.13. For normal rats, the absolute values of all responses are below 0.13. In the Discussion section, we will compare the average response for every rat in Figure 6a. A significant difference can be obtained when comparing the average responses of normal rats and of acute rats.

Verification of Breath Ammonia. To verify that the sensing response is due to breath ammonia, we utilize the following analysis methods: (1) Ion chromatography (IC) is used to detect breath of normal rat and breath of rat with liver injury. The IC method can analyze ammonia concentration with

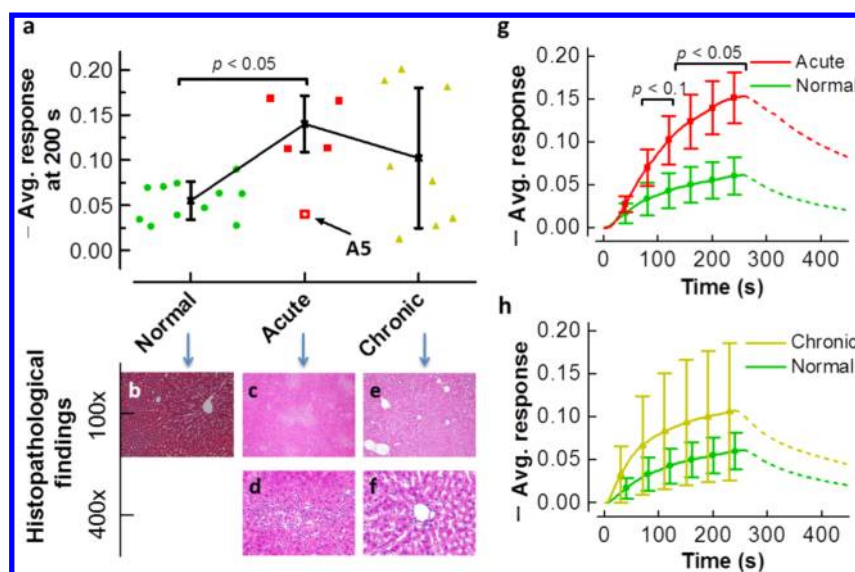


Figure 6. (a) Colored symbols represent average response of an individual rat in the normal group, acute group, or chronic group. Black symbols represent the average responses with standard deviations for the three groups. Panels b–f show hepatopathology alteration images of the normal group (b), acute group (c and d), and chronic group (e and f). Histological analysis revealed focal, moderate, acute necrosis, and hemorrhage with inflammatory cell infiltration in the central area of the liver tissue in 4/5 of the acute group. The hepatopathy was mild to moderate in the chronic group. (g) Average responses with standard deviations of the normal group and acute group as a function of sensing time. Dashed lines represent the responses after removing the breath of rats. The p -value is smaller than 0.05. (Kruskal–Wallis one-way ANOVA with Dunn’s post hoc analysis.) (h) Average responses with standard deviations of the normal group and chronic group as a function of sensing time.

an LOD around 100 ppb. (For IC, the LOD as 10 ppb is achievable if the volume of the gaseous sample is increased. However, here we use 250 s with a flow rate as 1.6 NL/min to collect breath of rats. The LOD of the IC method is only 100 ppb in this study.) (2) GC/MS is used to analyze the composition and the concentration of VOCs in rats’ breath. (3) A commercial ammonia filter can be inserted into our sensing system (as shown in Figure 3b) to check if the VNJ-P3HT diode’s response is eliminated or not.

The analyzed results by using IC and GC/MS are shown in Table 1 (see Supporting Information Table S-3 for more details).

Table 1. Chemical Composition/Concentration of the Breath of Rats by Using IC and GC/MS Analysis

compound	concn (ppb)		method
	normal	liver injury	
ammonia	<100	629.54	IC
ethanol	474.4	2769.6	GC/MS
isopropyl alcohol	68.4	43.8	GC/MS
isoflurane	48.1	63.1	GC/MS
acetone	36.7	131.3	GC/MS
toluene	7.1	16.1	GC/MS
acetonitrile	1.4	155.9	GC/MS

Using the IC method, we can tell that breath ammonia concentration of rat with liver injury is higher (629.54 ppb) than those of normal rats (<100 ppb). Comparing VOCs concentration, we also showed that the concentrations of acetone, ethanol, and acetonitrile are significantly increased for rats with liver disease. In Figure 4d, we have demonstrated that our sensor exhibits very small response to acetone and ethanol. The cooling step greatly suppresses the concentrations of VOCs with low vapor pressure at -20 °C. We also tested our sensor response to acetonitrile and found that the sensor only exhibits a small response (0.003) when acetonitrile concentration is 5 ppm

(data not shown). Hence, among ammonia, acetone, ethanol, and acetonitrile, only ammonia molecules dominantly react with the proposed sensor.

As shown in Supporting Information Figure S-2, when the sensing tube is switched to connect with an ammonia filter ($\text{NiCl}_2 \cdot 6\text{H}_2\text{O}$ powders) before entering the sensing chamber, the response is diminished (red line). When we disconnect the ammonia filter, we can again obtain clear and repeated response of rats as shown by black and green lines in Supporting Information Figure S-2. We therefore confirm that the sensing responses in this system refer to ammonia concentrations in the breath of rat.

Hepatopathology Alteration. Hepatopathology alteration image of normal rat is in Figure 6b. Those of acute group are shown in Figure 6, parts c and d. Those of chronic group are in Figure 6, parts e and f. Histological analysis reveals focal, moderate, acute necrosis, and hemorrhage with inflammatory cell infiltration in the central area of the liver tissue in 4/5 of the animals in the acute group. One animal (rat A5) in the acute group shows mild hepatic injury (histopathological alteration), and its breath ammonia response (indicated by the arrow in Figure 6a) is similar to those of the naïve rats. In the chronic group, the hepatopathy is mild to moderate.

DISCUSSION

We demonstrate a novel ammonia sensor based on a simple structure and low-cost process. Putting the sensor into a microfluid system, we obtain sensor response to breath of rats. In the following parts, we will discuss three major issues: (1) the reliability of the sensor, (2) the correlation between breath ammonia and the sensor response to rat, and (3) the sensor’s ability to differentiate between healthy rats and rats with hepatic injury.

Sensor device variation has been proved to be small as shown by the small error bars in Figure 4c. The sensor lifetime is verified by the following two experiments. First, when the background

ambient is nitrogen, the responses of a fresh VNJ-P3HT diode and of a 8 h aged VNJ-P3HT diode to 500 ppb ammonia are compared in Supporting Information Figure S-3a. Almost no degradation can be observed. Second, during breath ammonia testing, the responses as a function of time of a fresh VNJ-P3HT diode and of a 5 h aged VNJ-P3HT diode to 400 ppb ammonia are compared in Supporting Information Figure S-3b. The aged sample has been used to detect breath ammonia of rats for 12 times during 5 h. The variation of the response between the fresh sample and the aged sample is within 4%, verifying that the VNJ-P3HT diode is reliable enough for at least 5 h of operation.

Then, we discuss the correlation between breath ammonia and the sensor response to rat. According to literatures,^{2–5,23} the exhaled breath of rats with hepatic disease may contain a higher concentration of ammonia and several kinds of VOCs. In Table 1, using IC and GC/MS analysis, we also showed that the concentrations of ammonia, acetone, ethanol, and acetonitrile are significantly increased for rats with liver disease. As aforementioned, we have demonstrated that our sensor exhibits a very small response to acetone, ethanol, and acetonitrile. When using an ammonia filter to check the rat's response, the response disappears, verifying that the sensor response is due to the breath ammonia of rats (Supporting Information Figure S-2). Another question is about the contamination control. In previous studies on breath VOC testing of rats,^{22,24} for collecting breath samples, the trachea of rats was connecting to a tube directly to avoid contamination from oral or nasal cavities. Here in our study, we like to avoid risks of surgical complications; we collect breath by putting a mask to cover the rats' mouth and nose to simulate the clinical situation as shown by the picture in the inset of Figure 5. In our system containing a cooling step, most VOCs are greatly suppressed. Hence, contaminant VOCs from the oral or nasal cavity can be ignored. Ammonia generated from the oral cavity is mostly due to the metabolization of urea by bacteria in the gastrointestinal tract.^{37,38} (See Supporting Information: Generation of Breath Ammonia.) The increase of urea usually indicates injury in the kidney and may also lead to increased ammonia from the oral cavity. In this study, we aim to compare the breath ammonia concentration between healthy rats and rats with liver injury. There were no gross and microscopic lesions in kidneys (data not shown). Hence, increased ammonia concentration is not likely to be from the oral cavity. Breath ammonia collection by using the simple mask is acceptable. For future application, the proposed sensor is not used to identify disease, but to provide alert for patients with liver or kidney diseases. Breath ammonia from both the intraoral part and alveolar part needs to be considered.

After analyzing the sensor variation and sensor lifetime, we prove that the response deviation in Figure 5 is not due to the device degradation or variation. It is therefore suggested that the breath ammonia concentration of individual rat exhibits an obvious deviation, which agrees with the results in a previous report.¹²

The average response calculated from every rat, however, delivers an interesting message. In Figure 6a, the average responses (R_A) for normal, acute, and chronic rats are compared. For rats tested for only one time, the one-shot data are considered as their average response and are shown in Figure 6a. The average responses of rats in the acute group are much larger than the average response of rats in the normal group. According to the histological findings in Figure 6b–d, the significant large responses in acute rats correspond to moderate liver injury. The exceptional case in the acute group, rat A5, has small breath

ammonia response and it also corresponds to mild liver injury. For the chronic group, some rats deliver large breath responses (absolute value >0.1) and some still have small responses (absolute value <0.1). The average responses in the chronic group thus have a large deviation. Their hepatopathology alternation images in Figure 6, parts e and f, tell that the hepatopathy is mild to moderate.

Then, the average responses (R_A) obtained from individual rats as a function of sensing time are plotted in Figure 6, parts g and h. R_A of the acute group and normal group are compared in Figure 6g, while those of the chronic group and normal group are compared in Figure 6h. Rat A5 is not included in Figure 6g. The error bar represents the standard deviation caused by the distribution of average responses for different rats in one group. Using Kruskal–Wallis one-way ANOVA with Dunn's post hoc analysis, at a fixed 200 s sensing time, the significant difference of three groups is 0.039 and the significant difference between normal and acute groups is less than 0.05 as shown in Figure 6g. In Figure 6h, large responses between 0.1 and 0.2 are all from chronic rats. However, the difference between responses of chronic rats and normal rats is not significant.

These results demonstrate that, given an average sensor response value, our breath ammonia measurement may not be specific to distinguish between acute and chronic liver injury, but the average responses can reflect liver that undergoes acute–moderate injury. For those small breath ammonia responses in the chronic group, it might be because the hepatopathy is still mild. In future works, a longer experimental period for the chronic group will be applied to exam the breath ammonia response. Our next aim is to develop breath sensors to help patients with chronic hepatic disorders to trace their conditions. Since their clinical signs are usually vague, early or daily in-home monitoring may help these patients to detect the progress before severe hepatopathy. There are no existing literatures to report elevated breath ammonia for patients with early stage liver disease. However, in hepatic insufficiency, it is known that ammonia is not adequately detoxified and enters the systemic circulation. It is worthy to evaluate the possibility of monitoring early stage hepatic disorders by detecting breath ammonia. Since breath ammonia may reflect malfunctions in the liver, kidney, or oral cavity, a breath ammonia sensor itself cannot identify disease but can provide an alert signal to patients. Combining an ammonia sensor and VOC sensor to deliver a sensing map may help to identify disease in the future. However, more studies are required.

■ CONCLUSIONS

We proposed a new organic diode with vertical nanojunctions to detect the breath ammonia of rats. The proposed sensor exhibits high sensitivity, good enough selectivity, real-time and reversible response, and low production cost. We first demonstrated a direct comparison between breath ammonia and histological evaluation of liver tissue. For TAA-induced hepatopathy rats, we observe that a solid-state sensor can detect liver that undergoes acute, moderate hepatopathy. We also observe that, for one individual rat, the breath ammonia responses have a large deviation between several testings. The average response obtained from several testings of one rat, however, delivers an interesting signal. For rats in acute and normal groups, the average response of one rat is close to that of another rat in the same group. Moreover, the average response of rats in the acute group is significantly larger than the average response of rats in the normal group with a p -value smaller than 0.05.

This work aims for developing a breath ammonia sensor to provide daily in-home monitoring for patients with liver disease. Preliminary results in this work appear prospective. In future works, the response of our sensors to long-term chronic hepatic injury should be investigated, especially with respect to cirrhosis and liver tumors. We anticipate that the study facilitates the development of commercial low-cost breath analysis sensors and the investigation of sophisticated breath-ammonia-related disease models.

■ ASSOCIATED CONTENT

● Supporting Information

Introduction of generation of breath ammonia, comparison between various kinds of ammonia sensors, the plot of sensor response to study mixed gases effect, the table and plot to verify breath ammonia response of rat, and the plot of sensor response to confirm sensor lifetime. This material is available free of charge via the Internet at <http://pubs.acs.org>.

■ AUTHOR INFORMATION

Corresponding Author

*Phone: +886-3-513-1305 (H.-W.Z.); +886-2-2875-77181 (H.C.). Fax: +886-3-573-7681 (H.-W.Z.); +886-2-2875-7702 (H.C.). E-mail: hsiaowen@mail.nctu.edu.tw (H.-W.Z.); hc_cheng@vghtpe.gov.tw (H.C.).

Author Contributions

[†]M.-Z.D. and Y.-L.L. contributed equally to this work.

Notes

The authors declare no competing financial interest.

■ ACKNOWLEDGMENTS

This work was supported in part by the National Science Council under Grant NSC-100-2628-E-009-018-MY3 and in part by Veterans General Hospitals and University System of Taiwan Joint Research Program under Grants VGHUST100-G5-1-1 and VGHUST100-G5-1-3.

■ REFERENCES

- (1) Manolis, A. *Clin. Chem.* **1983**, *29*, 5–15.
- (2) Shimamoto, C.; Hirata, I.; Katsu, K. *Hepato-Gastroenterology* **2000**, *47*, 443–445.
- (3) Adrover, R.; Cocozzella, D.; Ridruejo, E.; Garcia, A.; Rome, J.; Podesta, J. J. *Dig. Dis. Sci.* **2012**, *57*, 189–195.
- (4) Van den Velde, S.; Nevens, F.; Van Hee, P.; van Steenberghe, D.; Quirynen, M. J. *Chromatogr., B* **2008**, *875*, 344–348.
- (5) DuBois, S.; Eng, S.; Bhattacharya, R.; Rulyak, S.; Hubbard, T.; Putnam, D.; Kearney, D. J. *Dig. Dis. Sci.* **2005**, *50*, 1780–1784.
- (6) Hibbard, T.; Killard, A. J. *Crit. Rev. Anal. Chem.* **2011**, *41*, 21–35.
- (7) Davies, S.; Spanel, P.; Smith, D. *Kidney Int.* **1997**, *52*, 223–228.
- (8) Kearney, D. J.; Hubbard, T.; Putnam, D. *Dig. Dis. Sci.* **2002**, *47*, 2523–2530.
- (9) Wang, T. S.; Pysanenko, A.; Dryahina, K.; Spanel, P.; Smith, D. J. *Breath Res.* **2008**, *2*, 037013.
- (10) Norman, M.; Spirig, C.; Wolff, V.; Trebs, I.; Flechard, C.; Wisthaler, A.; Schnitzhofer, R.; Hansel, A.; Neftel, A. *Atmos. Chem. Phys.* **2009**, *9*, 2635–2645.
- (11) Wang, J.; Zhang, W.; Li, L.; Yu, Q. *Appl. Phys. B: Lasers Opt.* **2011**, *103*, 263–269.
- (12) Hibbard, T.; Killard, A. J. *Breath Res.* **2011**, *5*, 037101.
- (13) Ishida, H.; Satou, T.; Tsuji, K.; Kawashima, N.; Takemura, H.; Kosaki, Y.; Shiratori, S.; Agishi, T. *Bio-Med. Mater. Eng.* **2008**, *18*, 99–106.
- (14) Becker, B.; Cooper, M. A. *J. Mol. Recognit.* **2011**, *24*, 754–787.

- (15) Aguilar, A. D.; Forzani, E. S.; Nagahara, L. A.; Amlani, I.; Tsui, R.; Tao, N. J. *IEEE Sens. J.* **2008**, *8*, 269–273.
- (16) Field, C. R.; In, H. J.; Begue, N. J.; Pehrsson, P. E. *Anal. Chem.* **2011**, *83*, 4724–4728.
- (17) Gong, J.; Li, Y. H.; Hu, Z. S.; Zhou, Z. Z.; Deng, Y. L. *J. Phys. Chem. C* **2010**, *114*, 9970–9974.
- (18) Jeong, J. W.; Lee, Y. D.; Kim, Y. M.; Park, Y. W.; Choi, J. H.; Park, T. H.; Soo, C. D.; Won, S. M.; Han, I. K.; Ju, B. K. *Sens. Actuators, B* **2010**, *146*, 40–45.
- (19) Ruzsanyi, V.; Baumbach, J. I.; Sielemann, S.; Litterst, P.; Westhoff, M.; Freitag, L. J. *Chromatogr., A* **2005**, *1084*, 145–151.
- (20) Toda, K.; Li, J.; Dasgupta, P. K. *Anal. Chem.* **2006**, *78*, 7284–7291.
- (21) Tisch, U.; Haick, H. *MRS Bull.* **2010**, *35*, 797–803.
- (22) Haick, H.; Hakim, M.; Patrascu, M.; Levenberg, C.; Shehada, N.; Nakhoul, F.; Abassi, Z. *ACS Nano* **2009**, *3*, 1258–1266.
- (23) Amal, H.; Ding, L.; Liu, B. B.; Tisch, U.; Xu, Z. Q.; Shi, D. Y.; Zhao, Y.; Chen, J.; Sun, R. X.; Liu, H.; Ye, S. L.; Tang, Z. Y.; Haick, H. *Int. J. Nanomed.* **2012**, *7*, 4135–4146.
- (24) Tisch, U.; Aluf, Y.; Ionescu, R.; Nakhleh, M.; Bassal, R.; Axelrod, N.; Robertman, D.; Tessler, Y.; Finberg, J. P. M.; Haick, H. *ACS Chem. Neurosci.* **2012**, *3* (3), 161–166.
- (25) Lin, P.; Yan, F. *Adv. Mater.* **2012**, *24*, 34–51.
- (26) Timmer, B.; Olthuis, W.; Berg, A. V. D. *Sens. Actuators, B* **2005**, *107*, 666–677.
- (27) Chen, C. T.; Chu, C. J.; Wang, T. F.; Lu, R. H.; Lee, F. Y.; Chang, F. Y.; Lin, H. C.; Chan, C. C.; Wang, S. S.; Huang, H. C.; Lee, S. D. J. *Gastroenterol. Hepatol.* **2005**, *20*, 450–455.
- (28) Kang, J. S.; Wanibuchi, H.; Morimura, K.; Puatanachokchai, R.; Salim, E. I.; Hagihara, A.; Seki, S.; Fukushima, S. *Toxicol. Sci.* **2005**, *85*, 720–726.
- (29) Mohammad, F. *J. Phys. D: Appl. Phys.* **1998**, *31*, 951–959.
- (30) Zan, H. W.; Tsai, W. W.; Chen, C. H.; Tsai, C. C. *Adv. Mater.* **2011**, *23*, 4237–4242.
- (31) Cassinelli, M. E. Method: 6016. In *NIOSH Manual of Analytical Methods*, 4th ed.; U.S. Department of Health, Education and Welfare: Washington, DC, 1996.
- (32) McClenny, W. A.; Holdren, M. W. Compendium Method TO-14A and TO-15. In *Compendium of Methods for the Determination of Toxic Organic Compounds in Ambient Air*, 2nd ed.; U.S. Environmental Protection Agency: Cincinnati, OH, 1999.
- (33) Nikitenko, V. R.; Heil, H.; von Seggern, H. *J. Appl. Phys.* **2003**, *94*, 2480–2485.
- (34) Brutting, W.; Berleb, S.; Muckl, A. G. *Org. Electron.* **2001**, *2*, 1–36.
- (35) Fukuda, H.; Yamagishi, Y.; Ise, M.; Takano, N. *Sens. Actuators, B* **2005**, *108*, 414–417.
- (36) Saxena, V.; Aswal, D. K.; Kaur, M.; Koiry, S. P.; Gupta, S. K.; Yakhmi, J. V.; Kshirsagar, R. J.; Deshpande, S. K. *Appl. Phys. Lett.* **2007**, *90*, 032516.
- (37) Center, S. A. Pathophysiology, Laboratory Diagnosis, and Diseases of the Liver. In *Textbook of Veterinary Internal Medicine*, 4th ed.; Ettinger, S. J., Feldman, E. C., Eds.; Elsevier-Saunders: Philadelphia, PA, 1995; Chapter 106, pp 1287–1289.
- (38) Bain, P. J. Liver. In *Duncan & Prasse's Veterinary Laboratory Medicine: Clinical Pathology*, 4th ed.; Latimer, K. S., Mahaffey, E. A., Prasse, K. W., Eds.; Iowa State Press: Ames, IA, 2003; Chapter 7, pp 206–208.